Electronic Materials Letters, Vol. 1, No. 1 (2005), pp. 47-52

In-Situ Magneto-Optical Kerr Effect Studies of Exchange-Bias Formations in Ferromagnetic/Antiferromagnetic Thin Film Systems

Young-Sang Yu, Ki-Suk Lee, Dong-Ju Jeon, Sang-Koog Kim*, Kwang Youn Kim[1], Seong-Ho Jang[2], Young-Woon Kim[2], Jeong-Woon Lee[3], and Sung-Chul Shin[3]

Nanospintronics Laboratory, School of Materials Science and Engineering, and Research Institute of Advanced Materials, Seoul National University, Seoul 151-744, Korea
[1]Advanced Metals Research Center, Korea Institute of Science and Technology, Seoul 136-791, Korea
[2]School of Materials Science and Engineering, Seoul National University, Seoul 151-742, Korea
[3]Center for Nanospinics of Spintronic Materials and Department of Physics, Korea Advanced Institute of Science and Technology, Daejeon 305-701, Korea

We report on experimental investigations of exchange-bias formations in different layered structures of Ta/NiFe/CoFe/Cu/CoFe/FeMn/Ta and Ta/NiFe/FeMn/Co by *in-situ* visible light magneto-optical Kerr effect. It is found that exchange bias (a kind of unidirectional anisotropy) can be controlled by aligning the magnetization orientations of ferromagnetic layers during cooling through the blocking temperatures, as well as by applying a suffcient magnetic field during the film growth. For the structure of a magnetic NiFe/FeMn/Co trilayer, oppositely oriented exchange bias of the two ferromagnetic NiFe and Co layers is found to be set with the single antiferromagnetic FeMn layer through the oppositely oriented remnant magnetizations of the two ferromagnetic layers while cooling. These results reveal that the exchange bias and its unidirectional orientation can be determined by interfacial uncompensated antiferromagnetic spins in contact with ferromagnets, which are locked in by the magnetization orientations of ferromagnets during the film growth or subsequent cooling.

Keywords: exchange bias, unidirectional anistropy, exchange bias formation

1. INTRODUCTION

When a ferromagnet (FM) is in contact with an antiferromagnet (AFM) and both layers are exchange-coupled, a shift of magnetization hysteresis loops is typically observed, which is called exchange bias. This effect is well known to be associated with a kind of unidirectional anisotropy newly formed at the interface of a coupled FM/AFM system[1–6]. Such a type of magnetic anisotropy was first discovered in fine particles of Co, with its surrounding oxide, by Meiklejohn and Bean (MB) in 1956[1]. Since then, the exchange bias phenomenon has been extensively and intensively studied in a variety of systems, including coupled FM/AFM bilayers. However, a comprehensive understanding of several aspects of the underlying physics is lacking with regard to various exchange bias behaviors that have been observed in experiments. For example, a generally accepted model suggested by MB explains that the origin of exchange bias behaviors is ascribed to exchange couplings between the AFM and FM layers in assumptions of a fully uncompensated state of interfacial AFM spins in a proximity to an FM and the rigidity of the AFM during the magnetization reversals of FM layers[1]. However, according to this model the strength of exchange bias field (H_{eb}) is predicted to be two orders of magnitude greater than the experimental values[2]. On the other hand, Mauri *et al*.,[3] Malozemo *et al*.,[4] Koon *et al*.,[5] Takano *et al*.,[6] and other researchers have proposed their own models that reconcile, to some extent, the experimental and theoretical values of H_{eb}. However, none of the proposed models can explain the process of exchange bias formations and the underlying mechanisms are not universal.

According to a possible scenario of the exchange bias effect, interfacial AFM spins play a crucial role in the unidirectional anisotropy of an FM, so that the magnetization of the FM is pinned by the direction of the interfacial uncompensated AFM spins through exchange interactions between the AFM and FM layers[1]. From a technological point of view, this effect is very useful as a core technology of spin-valve heads[7,8] together with giant magnetoresistance (GMR)[9] for reading information stored in ultrahigh-density magnetic

*Corresponding author: sangkoog@sun.ac.kr

storage media of up to 100 Gb/in^2, as well as a new-generation nonvolatile magnetoresistive random access memory[10]. Currently, hot issues in the technological applications of the exchange bias effect are how to achieve a thermal stability in a temperature range at which devices can function and how to enhance GMR values in practical devices[8,10]. It is thus necessary to study the mechanism of the exchange bias formation in detail from both fundamental and technological points of view.

To investigate the formation process of the exchange bias, two different types of multilayer samples of an FM/AFM/FM trilayer and a top spin valve structure were fabricated. These two samples were heated to temperatures above their own blocking temperatures in an ultrahigh vacuum (UHV) chamber, and then the magnetization directions of individual FM layers were controlled by applying an external magnetic field. Those samples were subsequently cooled to room temperature (RT) to examine their unidirectional anisotropies. *In-situ* magneto-optical Kerr effect[11] at a visible light wavelength was used to measure magnetization reversal loops of the samples in the UHV chamber.

2. EXPERIMENTAL PROCEDURES

The layered structures of the two different samples studied here are Ta/$Ni_{81}Fe_{19}$/$Co_{90}Fe_{10}$/Cu/$Co_{90}Fe_{10}$/$Fe_{50}Mn_{50}$/Ta and Ta/$Ni_{81}Fe_{19}$/$Fe_{50}Mn_{50}$/Co, which are schematically illustrated together with the thicknesses of the individual layers in Fig. 1. The former and latter samples are hereafter referred to as sample A and sample B, respectively. The $Ni_{81}Fe_{19}$, $Co_{90}Fe_{10}$, and $Fe_{50}Mn_{50}$ layers are denoted as NiFe, CoFe, and FeMn, respectively, for simplicity. The whole structure of sample A and a part of sample B, i.e., the structure of Ta/NiFe/FeMn, were fabricated onto Si wafers covered with a 1500-Å-thick SiO_2 layer by magnetron sputtering at an Ar pressure of 1-2 mTorr and with a base pressure of 5×10^{-8} Torr in a high vacuum sputtering chamber[12]. During the films' growth, a magnetic field of 100 Oe was applied in the film plane. As for sample B, a 35-Å-thick Co layer was grown on the sputter-grown FeMn layer using e-beam evaporation with a deposition rate of 0.76 Å/min under a pressure of 2×10^{-8} Torr in a different UHV chamber. Before the Co deposition, the FeMn surface was cleaned by Ar^+ ion sputtering at an incident angle of 45° for approximately 10 min with a kinetic energy of 1 keV. During the deposition of the Co layer, a magnetic field of 150 Oe was applied along the same field direction as that applied during the deposition of the NiFe/FeMn film.

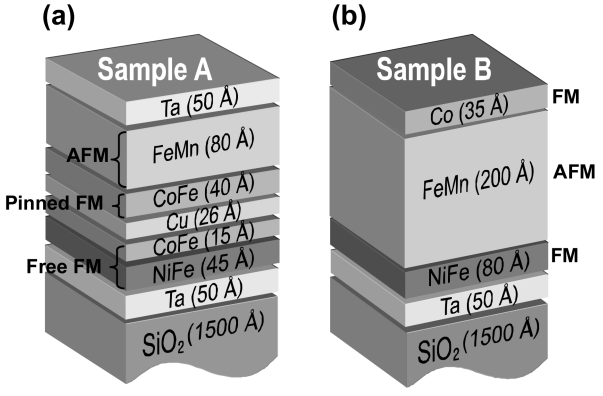

Fig. 1. (Color online) A schematic illustration of (a) a top spin valve structure (sample A), (b) a ferromagnetic/antiferromagnetic/ferromagnetic trilayer film (sample B).

Lateral uniformities of the grown samples were examined by a cross-section transmission electron microscope (TEM) and an energy dispersive spectroscope (EDS). Figures 2(a) and 2(b) show a typical cross section TEM image of sample B and the spatial mapping images of an EDS with the specificity of each constituent element. The root-mean-square roughnesses of the individual layers are much smaller than their thicknesses within the limit of a spatial resolution of less than nm. From the element-specific mapping images of EDS, the Co/Pd interface appears diffuse, due to its limited spatial resolution of greater than a few monolayers. The 15-Å thick Pd layer was prepared to protect against oxidation for its *ex-situ* characterizations. According to our previous experiments[13–15], the Co-Pd intermixing is about two monolayers thick. Similar structural interpretations are expected for sample A, because the same sputtering method and chamber were used to prepare both samples.

The magnetization reversal loops of the two samples were measured *in-situ* using the longitudinal magneto-optical

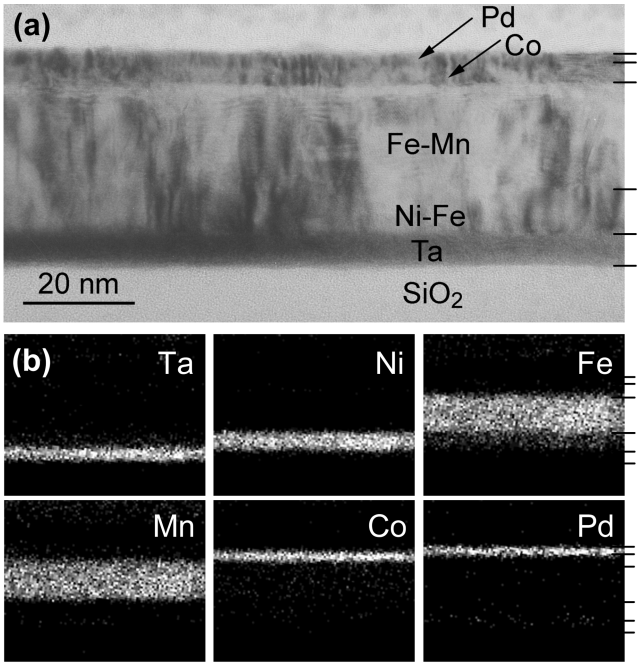

Fig. 2. (a) A cross-section TEM image, and (b) EDS spatial mapping images of sample B with a 15-Å thick Pd capping layer. The marked lines on the right edge indicate the interfaces between adjacent layers.

Kerr effect (MOKE) with a visible light wavelength. All the MOKE data of sample B were measured before the deposition of a Pd capping layer in a UHV chamber. The *in-situ* MOKE measurements have been described elsewhere in detail[16].

3. RESULTS AND DISCUSSION

Figure 3 shows typical magnetization M hysteresis and magnetoresistance curves of a spin valve film (sample A), *ex-situ* measured at RT using a vibrating sample magnetometer (VSM) and a four-point magnetoresistance probe, repectively. For those measurements, a magnetic field was applied along the field direction that was applied during the film growth. The reversal loop of a pinned CoFe layer in contact with the FeMn layer shows its shift by H_{eb} = -200 Oe. This indicates that the exchange bias at the CoFe/FeMn interface was set along the field direction applied during the film growth. In addition, the M reversal loop of a coupled NiFe/CoFe free layer is also shifted toward a negative field, H_{eb} = -7 Oe, which is associated with the pinned CoFe layer through an interlayer coupling between the free and pinned FM layers separated by a nonmagnetic spacer. This behavior has been understood based on either Néel coupling[17] or oscillating exchange coupling[18](for details, see Refs. 14, 15, 16). The MR curve related to these reversals is shown in Fig. 3(b).

To investigate how the exchange bias at FM/AFM interfaces is formed while cooling through the blocking temperature, we first determined the blocking temperature of the CoFe/FeMn interface of sample A. Kerr rotation loops were *in-situ* measured as a function of temperature ranging from 30 °C to 170 °C at an interval of 10 °C in an UHV chamber with field sweepings along the initial pinning direction, ϕ_{ip}, set during the film growth. Figure 4 shows some of those loops and the estimated values of H_{eb} and coercivity H_c(inset). At T = 130 °C, the exchange-biased loop is centered at zero field, but the coercivity continuously decreases even above T = 130 °C, and then reaches H_c=3.5 Oe at T =170 °C. Next, sample A was heated to 230 °C above the known blocking temperature, and then cooled to RT under a magnetic field of 300 Oe, which is sufficient to saturate the magnetizations of FM layers. Such field cooling was repeatedly performed on sample A by rotating the sample orientation with respect to the fixed magnets and the plane of incidence of a laser light for longitudinal MOKE measurements, as shown in Fig. 5(a). Thus, three different orientations of the applied magnetic field can be made with respect to ϕ_{ip} (i.e., ϕ_B =0 and 90 ° along the film plane and in the film normal) in order to reset unidirectional anisotropy, as shown in the left column of Fig. 5(b). After cooling from the different settings of exchange bias as described, Kerr rotation loops were measured with two different field sweepings, ϕ_R = 0 and 90 ° at RT.

For the sample with an exchange bias setting at ϕ= 0 (i.e., ϕ_{ip} is parallel to the fixed orientation of magnets), the RT Kerr rotation loop measured along ϕ_R = ° 0 shows H_{eb} = 170 Oe. On the other hand, the reversal loop for ϕ_R = 90 ° is not exchange-biased and shows a typical hard-axis loop. For an exchange bias setting with ϕ_B = 90°, the RT loop at ϕ_R = 90 ° shows H_{eb} = -160 Oe, while a hard-axis loop is observed at ϕ_R = 0 °. One more setting of exchange bias at ϕ_B = 0 ° maintains the same results shown in the first row of Fig. 5(b), indicating that the unidirectional anisotropy is recovered back to the initial pinning direction, i.e., ϕ_p. In the third row

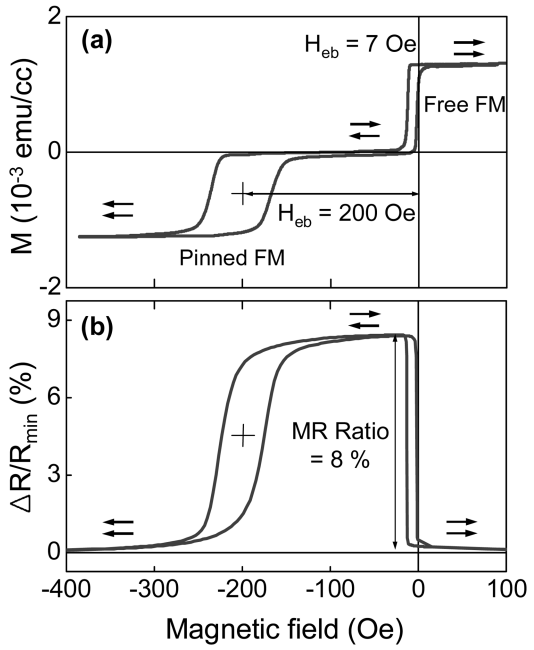

Fig. 3. (a) A hysteresis loop *ex situ* measured at room temperature by a VSM and (b) a magnetoresistance curve from sample A.

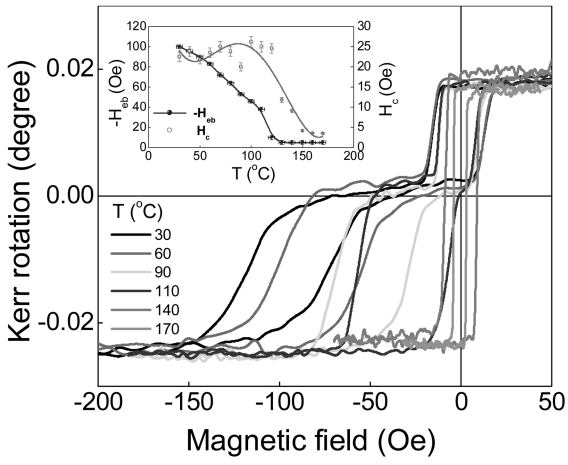

Fig. 4. (Color online) Kerr rotation loops of sample A measured at various temperatures, as noted. The inset shows H_{eb} and H_c versus temperature estimated from the reversal loops shown.

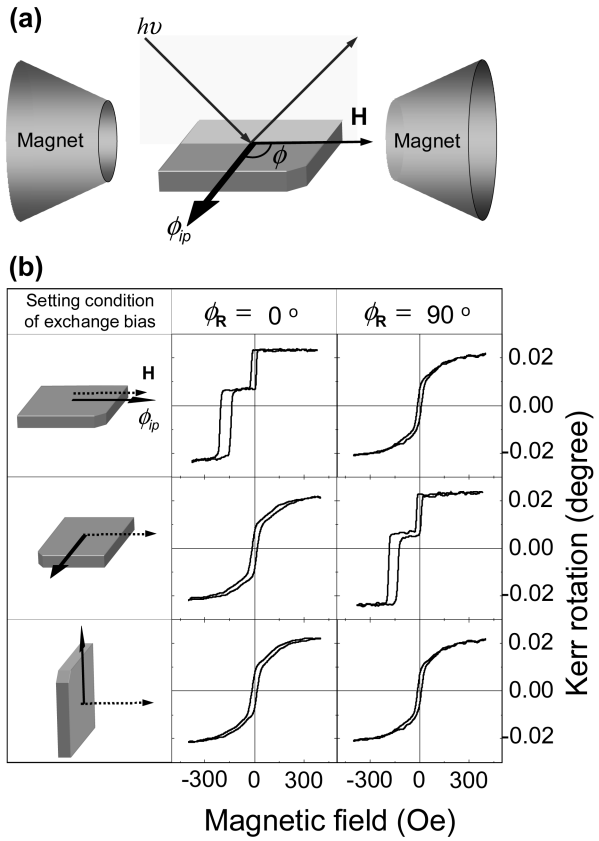

Fig. 5. (Color online) (a) An illustration of the geometry of longitudinal MOKE measurements and relative orientations ϕ between the sample and the applied field direction. ϕ_{ip} indicates the initial pinning direction set during the film growth. (b) In the left column are displayed the relative orientations between the sample and the field direction applied at an elevated temperature of 230 °. The second and last columns show Kerr rotation loops measured at RT at ϕ_R = 0 ° and 90 °, respectively, after exchange bias settings, as noted in the left column.

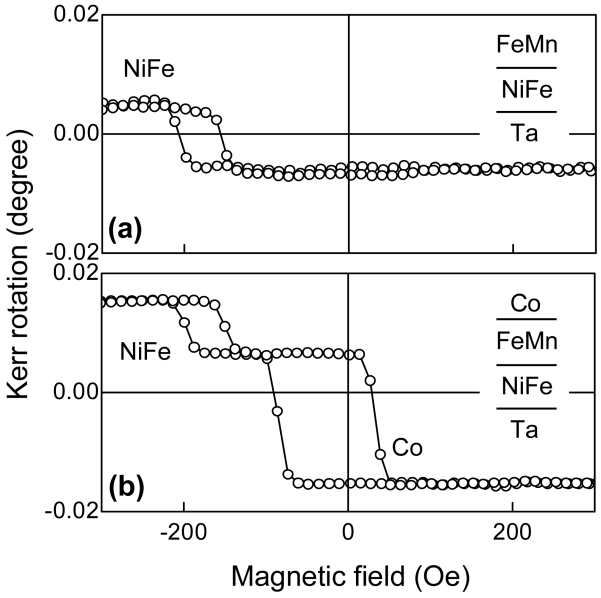

Fig. 6. Kerr rotation loops of the as-grown NiFe/FeMn in (a) and the NiFe/FeMn/Co trilayer in (b), measured at RT in a UHV chamber. H_{eb} and H_c values for the individual reversal loops are estimated to be H_{eb} = -180° and H_c = 27 Oe in (a), H_{eb} = -170 and H_c = 24 Oe for the NiFe reversal, and H_{eb} = -22 and H_c = 60 Oe for the Co reversal in (b).

of Fig. 5(b), the applied field direction for an exchange bias setting is normal to the film plane (We could not check if the exchange bias is set along the film normal); in this case, both loops at ϕ_R =0 ° and 90 ° exhibit no exchange bias effect, indicating that unidirectional anisotropy was not set in the film plane. From these results, we can learn how the pinning direction of an AFM layer is determined at the early stages of exchange-bias formations during cooling by the orientations of applied magnetic fields. In our earlier work[20–22], it is found that the pinning direction is associated with interfacial uncompensated AFM spins in proximity to an FM, although canted compensated AF spins can also yield similar exchange bias effects according to other models[5,23].

In general experiments, an external magnetic field has been applied during the film growth or various field-cooling procedures in order to lock in an exchange bias in coupled FM/AFM systems. In an alternative way, we can lock in an exchange bias by a cooling through its blocking temperature while holding a remanence state of the magnetizations of FM layers in an FM/AFM/FM trilayer structure. For the as-grown FeMn/NiFe film without Co, H_{eb} = -180 Oe and H_c = 27 Oe are observed, as shown in Fig 6(a). For the Co-grown film onto the NiFe/FeMn film, the Co exchange bias is observed to be H_{eb} = -22 Oe and H_c = 60, while keeping the exchange bias of NiFe unchanged, as shown in Fig. 6(b). The exchange biases of both the Co and NiFe layers were initially formed during the film growth by their individual magnetizations saturated along an applied magnetic field.

With sample B, we investigated how exchange bias is newly introduced by the remnant magnetization states of the two different FM layers under no applied magnetic field during cooling from 190 °C higher than its blocking temperature in a UHV chamber. First, a Kerr rotation loop was measured at 190 °C, as shown in Fig. 7(a). As expected, neither the Co layer nor the NiFe layer shows any loop shift. In contrast, a two-step symmetric hysteresis loop is observed because of the coercivity difference between the two FM layers. At this elevated temperature, antiparallel orientations of the magnetizations of the Co and NiFe layers can be achieved at applied fields in the two plateau regions indicated by the insets of i) and ii) in Fig. 7(a). The antiparallel orientations between the two F layers can be kept by applying magnetic fields sufficient to saturate both F layers at either left or right direction and then applying weak fields opposite to the previous saturation fields, based on the coercivity difference between Co and NiFe at the elevated temperature. Thus, the Co and NiFe layers are kept antiparallel during cooling through the blocking temperature, because the remnant mag-

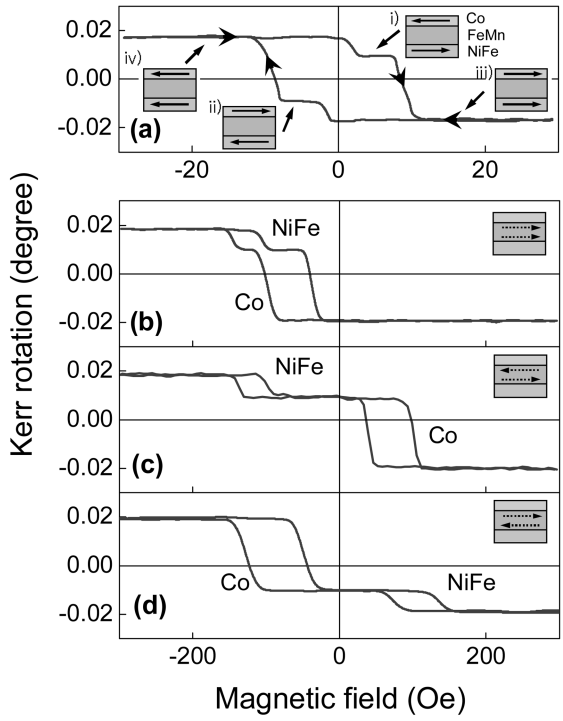

Fig. 7. (Color online) Kerr rotation loops of a NiFe/FeMn/Co trilayer film measured in a UHV chamber. The loop shown in (a) was measured at 190 °C, while the other loops in (b), (c), and (d) were measured at RT just after cooling through 190 °C, while maintaining the magnetization directions of the individual ferromagnetic layers as indicated by arrows in the insets of iii), i), and ii), respectively. The dashed arrows in the insets of (b), (c), and (d) represent the pinning directions of interfacial uncompensated antiferromagnetic spins that were locked in. H_{eb} and H_c values for those individual loops are given as follows: for the NiFe reversal, H_{eb} = -65 and H_c = 30 Oe in (b), H_{eb} = -120 and H_c = 20 Oe in (c), and H_{eb} = 110 and H_c = 31 Oe in (d); for the Co reversal, H_{eb} = -65 and H_c = 30 Oe in (b), H_{eb} = 73 and H_c = 31 Oe in (c), and H_{eb} = -85 and H_c = 39 Oe in (d).

netizations of the Co and NiFe along the easy axis are kept antiparallel in the two plateau regions even after the magnetic field is removed. After cooling with the different states indicated by the insets of i), ii), and iii), the Kerr loops measured at RT are shown in Figs. 7(c), 7(d), and 7(b), respectively. In Fig. 7(b), the negative field shifts of both Co and NiFe loops are observed, revealing the same orientation of their unidirectional anisotropy. Differences in the exchange bias and the coercivity between the loops shown in Figs. 6(b) and 7(b) are likely caused by different spin structures at the FM/AFM interface formed by the two different ways of the exchange bias setting during the film growth and the subsequent cooling through a blocking temperature. In contrast, with the same orientation of the unidirectional anisotropy, oppositely oriented exchange basing is also obtained with the single FeMn layer, after cooling, while maintaining the antiparallel remnant magnetizations between the Co and NiFe layers, as shown in Figs. 7(c) and 7(d). We can learn from these results that exchange bias is associated with uncompensated AFM spins localized at the corresponding interface with a proximal FM layer, whose direction is set by the magnetization direction of the proximal FM layer while cooling through the blocking temperature. In an earlier work of Nogues *et al.*,[24] a positive unidirectional exchange bias was also observed in an FeF_2/Fe bilayer system, indicating that AF spins are coupled to an external magnetic cooling field and the FeF_2Fe interaction is antiferromagnetic above the Néel temperature.

4. CONCLUSIONS

In the present work, we fabricated two different kinds of samples: a top spin valve of Ta/$Ni_{81}Fe_{19}$/$Co_{90}Fe_{10}$/Cu/$Co_{90}Fe_{10}$/$Fe_{50}Mn_{50}$/Ta and a magnetic trilayer film of Ta/$Ni_{81}Fe_{19}$/$Fe_{50}Mn_{50}$/Co. Using these two samples, we investigated how exchange bias is formed by different cooling procedures by employing *in-situ* magneto-optical Kerr effect with a visible wavelength in a vacuum chamber. From the observed experimental results, we conclude the following: 1) The orientation of unidirectional anisotropy formed in a coupled FM/AFM bilayer equals the direction of a magnetic field applied during the film growth, as well as during the field cooling through a blocking temperature. 2) When an FM/AFM bilayer is cooled from above its blocking temperature, while maintaining a remnant magnetization of the FM layer, the unidirectional anisotropy is introduced along the direction of the remnant magnetization. 3) For an FM/AFM/FM trilayer structure, when cooled through its blocking temperature, while maintaining antiparallel remnant magnetizations of the two FM layers, their unidirectional anisotropies are set as antiparallel with each other, driven by the remnant magnetization orientations of the individual proximal FM layers.

ACKNOWLEDGMENT

This work was supported by the Korea Research Foundation Grant (KRF-2002-003-D00137).

REFERENCES

1. W. C. Meiklejohn and C. P. Bean, *Phys. Rev.* **102**, 1413 (1956).
2. R. Jungblut, R. Coehoorn, M. T. Johnson, J. Van de Stegge, and A. Reinders, *J. Appl. Phys.* **75**, 6659 (1994).
3. D. Mauri, H. C. Siegmann, P. S. Bagus, and E. Kay, *J. Appl. Phys.* **62**, 3047 (1987).
4. A. P. Malozemo, *Phys. Rev. B* **35**, 3679 (1987).
5. N. C. Koon, *Phys. Rev. Lett.* **78**, 4865 (1997).
6. K. Takano, R. H. Kodama, A. E. Berkowitz, W. Cao, and G. Thomas, *Phys. Rev. Lett.* **79**, 1130 (1997).

7. J. C. S. Kools, *IEEE Trans. Magn.* **32**, 3165 (1996).
8. C. Tsang, *J. Appl. Phys.* **55**, 2226 (1984).
9. M. N. Baibich, J. M. Broto, A. Fert, F. Nguyen Van Dau, F. Petro, P. Eitenne, G. Creuzet, A. Friederich, and J. Chazelas, *Phys. Rev. Lett.* **61**, 2472 (1988).
10. W. H. Butler, X. -G. Zhang, T. C. Schulthess, D. M. C. nicholson, and A. B. Oparin, *J. Appl. Phys.* **85**, 5834, (1999).
11. Z. Q. Qiu and S. D. Bader, *J. Magn. Magn. Mat.* **200**, 664 (1999).
12. K. Y. Kim, K. S. Shin, S. H. Han, S. H. Lim, H. J. Kim, S. H. Jang, and T. Kang, *Korean Magn. Soc.* **10**, 67 (2000).
13. S.-K. Kim, Y. M. Koo, V. A. Chernov, and H. Padmore, *Phys. Rev. B* **53**, 11114 (1996).
14. S.-K. Kim, Y. M. Koo, V. A. Chernov, J. B. Kortright, and S.-C. Shin, *Phys. Rev. B* **62**, 3025 (2000).
15. S. -K. Kim and S.-C. Shin, *J. Appl. Phys.* **89**, 3055 (2001).
16. J.-W. Lee, J. Kim, S.-K. Kim, J.-R. Jeong, and S.-C. Shin, *Phys. Rev. B* **65**, 144437 (2002).
17. L. Néel, *Comptes. Rendus* **255**, 1676 (1962).
18. R. Coehoorn and J. P. W. B. Duchateau, *Phys. Rev. B* **44**, 9331 (1991).
19. J. C. S. Kools and W. Kula, *J. Appl. Phys.* **85**, 4466, (1999).
20. S.-K. Kim, K.-S. Lee, J. B. Kortright, and S.-C. Shin, *Appl. Phys. Lett.* **86**, 102502 (2005).
21. K.-S. Lee, Y.-S. Yu, and S.-K. Kim, *Appl. Phys. Lett*. **86**, 192512 (2005).
22. K.-S. Lee, S.-K. Kim, J. B. Kortright, K. Y. Kim, and S.-C. Shin, *J. of Magnetics* **10**, 36-39, (2005).
23. Y. Sakurai and H. Fujiwara, *J. Appl. Phys.* **93**, 8615 (2003).
24. J. Nogues, D. Lederman, T. J. Moran, and I. K. Schuller *Phys. Rev. Lett.* **76**, 4624 (1996).